Behavior of Yarn Pullout from Woven Fabrics: Theoretical and Experimental

NING PAN AND MEE-YOUNG YOON

Division of Textiles and Clothing, University of California, Davis, California 95616, U.S.A.

ABSTRACT

Yarn pullout behavior from a woven fabric is an important indicator of the mechanism of yarn interactions within the fabric and a predictor of its various mechanical properties. It is investigated in this paper both theoretically and experimentally. An analytical model developed for nonwoven structures is modified here to describe the yarn pullout process. This theory is able to predict the relationship of the maximum pullout load and the embedded yarn length in a woven fabric with tight structure. The maximum load is shown in the theory related to the mechanical and geometric properties of the fabric and yarn. Experimental work verifies the connections between fabric properties and yarn pullout behavior, and a comparison of critical yarn pullout lengths, predicted and measured, is also presented. This work should be useful in understanding the nature of yarn interaction in a fabric as well as the structure-reinforcing mechanism of woven fabrics.

Textile testing serves the purpose of characterizing the properties (or qualities) of textile products: for instance, uniaxial fabric tensile testing provides information about behavior under uniaxial tensile load, whereas the fabric response towards a compressional load is revealed by a compressional test. Along with the development of new products and the need to better understand the performance and behavior of these products, new developments of textile testing in both scope and methodology are also emerging; they are expected to offer new or more accurate information about textile structures.

Among all textile products, woven fabric is probably the most used. It has a unique structure, which in most cases consists of yarns in two systems perpendicular to and interlaced with each other to form a system with certain strength. The interlacing (or crossing) points are the major locations where interactions between yarns in the two systems take place and through which the yarns form an interlocked structure. Without this interaction at the interlacing points, a woven fabric would be equivalent to sheets made of parallel but isolated yarns; the resultant properties would be entirely different from a practical fabric. In other words, this yarn interaction at the crossing points is the essential feature of woven fabric and will affect more or less all the fabric properties. Therefore, yarn interaction at the crossing points can be used as an indicator or probe of various fabric properties, and such interaction can be examined through a single yarn pullout test from the fabric.

Taylor [13] is probably the first person who analyzed the role of yarn pullout on fabric properties. He developed a theory relating yarn interaction at crossing points to fabric tear strength and made actual yarn pullout tests. His work is a thorough experimental investigation of tensile and tear strengths of woven fabric, but his theory is to a large extent a semi-empirical one with no direct inclusion of such critical parameters as yarn mechanical and dimensional properties. Sebastian *et al.* [11, 12] also used the yarn pullout technique to evaluate the effect of a softening agent on fabric performance, and they proposed a simple model to calculate pullout load and the influence of yarns crossing over. The concept of using the yarn pullout method to investigate fabric properties is therefore not really novel, but the nature or mechanism of this interaction is still poorly understood and no study has focused on it.

In a fiber composite study, on the other hand, the single fiber pullout test has been used as one of the most fundamental experimental approaches by which one can analyze such issues as the nature of the interphase formed between fibers and the matrix material, the transfer of stress from matrix to fibers, and the strength and fracture of composites. The results of fiber pullout experiments have provided rich information to characterize interactions between fibers and matrix. There are numerous publications on this topic, and a few representative papers [1, 3, 4, 6] are provided in the reference list. Inspired by this method in a composite study, one of us (Pan [9]) proposed that the fiber pullout test and the theoretical analysis be used

for a similar purpose—to study bonded fiber structures such as nonwoven materials. Pan [9] demonstrated that such a study can predict the behavior of fiber pullout in these systems, provide insights on interactions between fibers by means of bonds, characterize bond properties, and reveal and estimate important parameters. For the same reason, the nature of yarn interactions at the interlacing points can be investigated through a yarn pullout test from the fabric.

Although there are significant differences between nonwoven and woven structures, Pan's theoretical model [9] can easily be applied to a woven fabric with appropriate modifications. First of all, a woven fabric is strengthened through the mechanical and frictional interactions between yarns at the crossing points, while a nonwoven is reinforced through the chemically bonded points between fibers. In other words, the nature of the interactions is different in the two cases. Also, in a woven fabric, all constituents (yarns) are arranged in only two (warp and weft) orthogonal directions and interlaced with each other at right angles, whereas in a nonwoven system, fibers orient and cross over each other in a much more complicated manner. Therefore Pan's theory [9] has to be modified to reflect these differences.

In this article, we first apply the modified theory to the yarn pullout process to reveal the effect of yarn interactions in fabrics, then we show the applications of this pullout technique in characterizing fabric mechanical behavior. Furthermore we also explore the connections between yarn pullout behavior and various fabric mechanical properties.

Theoretical Aspects

A portion of a plain weave fabric structure and an interlacing point on it are illustrated in Figure 1. From the figure, we see that the geometry of a crossing point can be characterized using such parameters as yarn thickness t_y, width w_y, and cross-sectional area A_y. If we consider the cross section of the yarn as an ellipse with major axis w_y and minor t_y, then we have

$$A_y = \pi t_y w_y \quad . \tag{1}$$

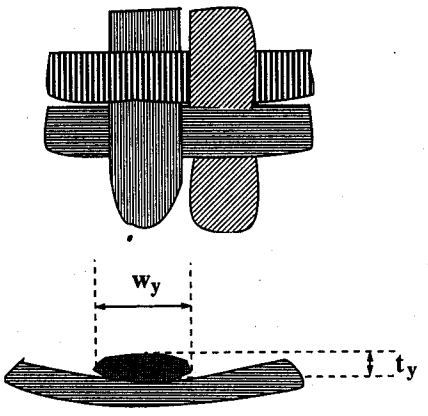

FIGURE 1. A plain weave and the geometry of the crossing point.

In any discrete fibrous system, the external load cannot be applied directly to all constituents simultaneously. Rather, it has to be transferred through a shear or frictional mechanism from one constituent to another. This is why the so-called shear lag theory, first proposed by Cox [2], governing this stress transfer process plays such an important role that almost all fiber pullout models in composite studies are based on it. The yarn pullout model in this paper, a modification of the theory proposed by Pan [9] for fiber pullout behavior from a nonwoven fabric, is also a shear lag type, so the major assumptions associated with the shear lag theory have to be adopted. First, during the yarn pullout process, the extensional stress in the fabric region (formed by the adjacent yarns) is negligible relative to that in the yarn. As a result, the distortion in the fabric due to yarn pullout (the fabric jamming effect) is small and can be excluded in the analysis. We have to admit that this assumption is highly idealized, and the actual local effects are often quite severe. So this theory applies more appropriately to fabrics with very tight structures. In addition, if there were no yarn interlacing at all, the yarn being pulled out would not develop tension within; it is the other yarns interlaced with it that offer restraint through a shear mechanism to stretch the yarn. We therefore assume the axial tension in the yarn being pulled out is the dominant action, and the shear stress in it is negligible compared to that in the crossing yarns. Also excluded are the effects of Poisson's ratios for both the yarn and fabric during the pullout process, so that the nature of yarn interaction will remain unchanged during the process.

Furthermore, during the yarn pullout process, there are two kinds of interactions between yarns occurring at the crossing points: frictional slippage and elastic interaction. In the former case, the analysis will become very simple. As long as the pressure at the crossing points is low and keeps constant, yarn pullout force will be a constant in a fabric where the yarn surface characteristics or frictional behaviors are given; that is, the force will be largely independent of the embedded yarn length as well as other yarn properties. Consequently, the results will not be very informative. Our analysis therefore focuses on the case where elastic interaction takes place between yarns. This occurs again in the fabrics with tight structures, so that the pressure

and interyarn friction at the crossing points are high. As a result, interyarn friction will provide enough restraint for the elastic interaction to take place, so the shear lag theory is applicable.

If we adopt Pan's analysis [9] with certain modifications to suit our present structure, the maximum force P_m pulling a yarn out of a single crossing point in a fabric can be expressed as

$$P_m = \frac{\tau_s w_y}{\rho} \tanh \rho w_y \quad , \tag{2}$$

where τ_s is the equivalent shear strength of the crossing point and ρ is a factor,

$$\rho = \sqrt{\frac{G_y}{E_y} \frac{w_y}{\pi A_y t_y}} = \frac{1}{t_y} \sqrt{\frac{G_y}{\pi E_y}} \quad , \tag{3}$$

with E_y being the tensile modulus of the yarn being pulled out and G_y the corresponding shear modulus of the cross-over yarns.

For a yarn in the fabric system with embedded length L, the total maximum pullout force becomes

$$P_{lm} = Int(n_y L) \frac{\tau_s w_y}{\rho} \tanh \rho w_y \quad , \tag{4}$$

where n_y is the corresponding fabric count (number of yarns per unit fabric length), and $Int(\ )$ is the integer function that omits the fraction part of the result and yields only an integer so as to reflect discrete crossing points. The equation shows clearly that for a given embedded yarn length, the single yarn pullout force is a function of fabric count and yarn dimensional and mechanical properties.

On the other hand, whether an embedded yarn can be completely pulled out from the fabric or will break within depends on both embedded length and yarn tensile strength. Thus a critical yarn length $L = L_c$ can be calculated according to the equilibrium on the yarn,

$$P_{lm} = P_{lu} = \sigma_{yu} A_y \quad , \tag{5}$$

where P_{lu} is the yarn breaking load and σ_{yu} is the yarn tensile strength.

We should point out here that, in practice, this critical yarn length will not be a constant; it changes due to the resulting structural distortion ignored in this analysis. This value will also vary depending on yarn type; Realff *et al.* [10] revealed that different yarn types follow distinct failure mechanisms. This, however, can be reflected by using the yarn parameters corresponding to a specific yarn type in the model. In the following discussion, we focus on the ring-spun yarns whose mechanical properties were provided by Pan [8].

Calculation and Discussion

Predicting Yarn Pullout Behavior

Among all the parameters involved, the geometric properties of a crossing point such as yarn thickness t_y, width w_y, and cross-sectional area A_y are measurable and can hence be considered as known. On the other hand, the yarn tensile modulus E_y and shear modulus G_y can be calculated using equations provided by Pan [8] once the fiber properties and yarn twist are given. In the present case, since we are only concerned with the ratio of these two moduli in calculating the factor ρ from Equation 3, it is much easier to use the information in reference 8 just to estimate the range of $\frac{G_y}{E_y}$. So the only parameter remaining unknown in the equations above is the equivalent shear strength τ_s of the crossing point. This parameter is difficult to measure but can be estimated based on the yarn pullout experiment. There are two ways to estimate τ_s. One is to directly use Equation 4 where all variables involved are known except the pullout load P_{lm} and τ_s. So once we obtain P_{lm} through a pullout test, we can calculate the τ_s value for that particular fabric from Equation 4. In some cases, it is preferable to use the slope equation provided below. We can differentiate Equation 4 to give

$$\frac{dP_{lm}}{dL} = Int(n_y) \frac{\tau_s w_y}{\rho} \tanh \rho w_y \quad . \tag{6}$$

That is, the slope of the curve of the pullout force versus the embedded yarn length is a constant for a given fabric as long as all the properties involved remain constant. So again based on the experimental results, once we know the slope of the pullout curve, we can calculate the value for τ_s.

As applied in reference 9, several nondimensional quantities are defined here for the convenience of discussion. First of all, because the product $\frac{\tau_s w_y}{\rho}$ in the equations above has the force unit, we can define a nominal restraint force of one crossing point as

$$g_y = \frac{\tau_s w_y}{\rho} \quad . \tag{7}$$

Equation 2 therefore suggests that because of limited yarn interlace length equal to yarn thickness w_y, the pullout force P_m per crossing point is discounted by an efficiency factor,

$$\eta_y = \tanh \rho w_y \quad , \tag{8}$$

compared to the restraint force g_y exerted on the yarn

due to the mechanism of stress transfer through the crossing point. When the contact length w_y approaches infinity, this discount will diminish as $\eta_y \rightarrow 1$.

Figure 2 depicts the effects of both modulus ratio $\frac{G_y}{E_y}$ and yarn ellipticity $\frac{w_y}{t_y}$ on the efficiency factor η_y. In general, when yarns are stiff in shear or a yarn's tensile modulus is low or the yarn width-thickness ratio is high, the crossing point will transmit stress more efficiently, reflected by a higher η_y value.

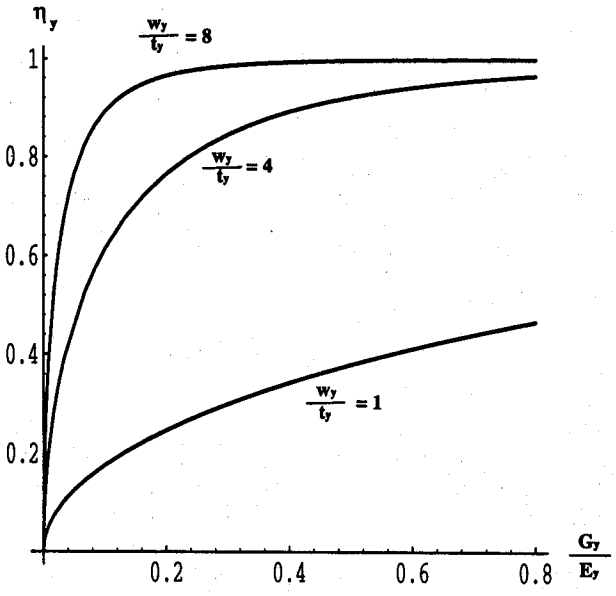

FIGURE 2. Effects of $\frac{G_y}{E_y}$ and $\frac{w_y}{t_y}$ on the efficiency factor η_y.

Equation 4 can be rewritten in terms of yarn tensile stress σ_y according to

$$P_{lm} = Int(n_y L)\frac{\tau_s w_y}{\rho}\eta_y = A_y\sigma_y \quad . \qquad (9)$$

Defining a dimensionless quantity $\frac{\sigma_y}{\tau_s}$ and rewriting Equation 9, we get

$$\frac{\sigma_y}{\tau_s} = Int(n_y L)\frac{\eta_y}{\pi t_y \rho} \quad . \qquad (10)$$

This gives a nondimensional or more general relationship between the relative pullout stress $\frac{\sigma_y}{\tau_s}$ and the embedded fiber length L as well as the yarn properties.

Figures 3 and 4 are plotted using this equation for a parametric study about the effects of the important factors involved, such as the moduli ratio $\frac{G_y}{E_y}$ and yarn cross section ellipticity $\frac{w_y}{t_y}$ based on Equation 10. Here we have used an embedded yarn length of $L = 0.6$ cm and a fabric count of $n_y = 10/\text{cm}$.

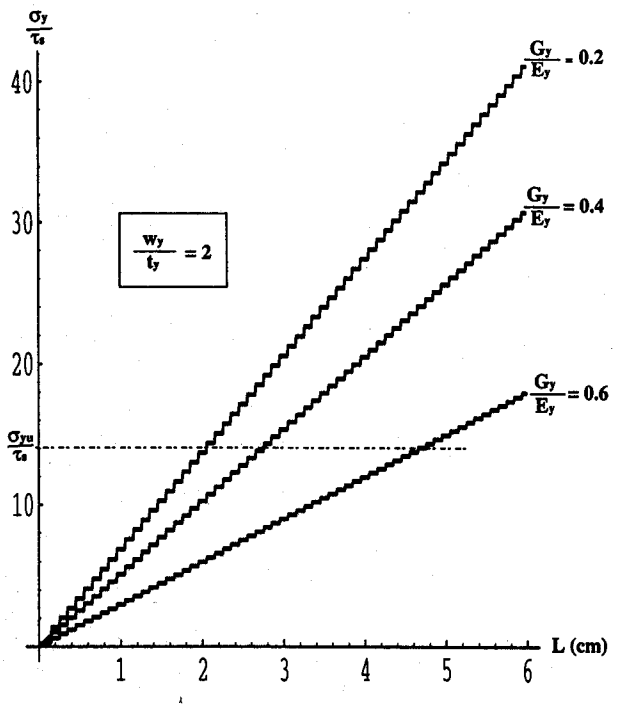

FIGURE 3. Relationship of the relative pullout stress and embedded yarn length at different $\frac{G_y}{E_y}$ levels.

Figure 3 shows the influence of $\frac{G_y}{E_y}$ on the relative pullout curve at a given ellipticity $\frac{w_y}{t_y} = 2$. The curve reveals that for a given yarn cross sectional area, the moduli ratio $\frac{G_y}{E_y}$ has a significant effect on the pullout process: a higher $\frac{G_y}{E_y}$ value, representing a yarn stiffer in shear or lower in tensile modulus, will result in lower relative stress.

On the other hand, the effect of ellipticity $\frac{w_y}{t_y}$ of the yarn cross section on pullout force is less significant, as shown in Figure 4, where ellipticity $\frac{w_y}{t_y}$ is allowed to alter at three different levels while the moduli ratio is

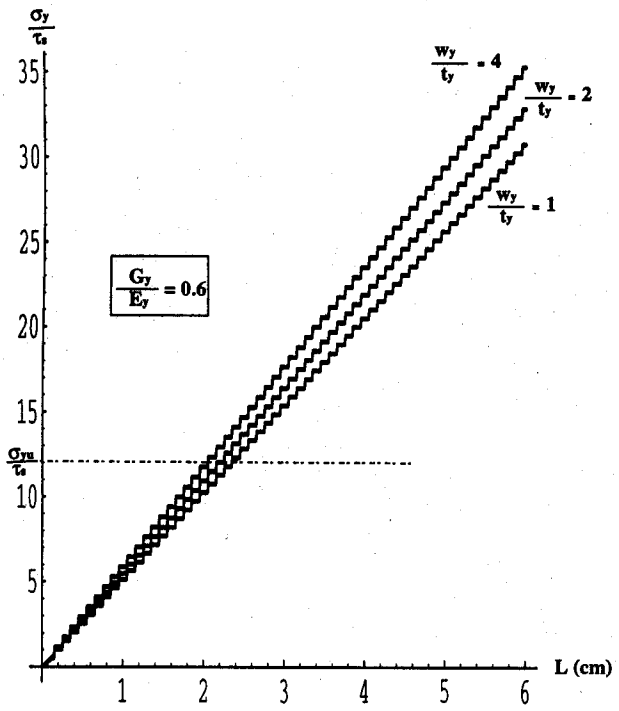

FIGURE 4. Relationship of the relative pullout stress and embedded yarn length at different $\frac{w_y}{t_y}$ levels.

kept a constant $\left(\frac{G_y}{E_y} = 0.6\right)$. It shows that in this case, a greater $\frac{w_y}{t_y}$ value, meaning a flatter yarn, will lead to higher relative stress.

The actual pullout stress is limited, however, to the value when the yarn tensile stress σ_y reaches its tensile strength σ_{yu}, as illustrated in the figures. As we stated above, this limit in turn defines a critical yarn length L_c beyond which the yarn will break inside the fabric rather than be pulled out. This critical yarn length L_c can also be expressed explicitly using Equation 10 as

$$L_c = Int\left(\frac{\sigma_{yu}}{\tau_s}\frac{\pi t_y \rho}{\eta_y} n_y\right) \quad . \qquad (11)$$

Since this equation has evolved from Equation 10, the effects of both moduli ratio $\frac{G_y}{E_f}$ and ellipticity $\frac{w_y}{t_y}$ on the value of this critical length L_c can be seen directly from Figures 3 and 4 if we replace the yarn tensile stress σ_y with its tensile strength σ_{yu}. In a later section, we will compare this prediction of yarn pullout critical lengths with experimental results.

CONNECTIONS BETWEEN PULLOUT AND FABRIC MECHANICAL PROPERTIES

As we mentioned in the beginning, because of the importance of yarn interaction at the crossing points to fabric structure, yarn pullout behavior should reflect various aspects of the mechanical properties of fabrics. To verify it, we have selected fifteen fabrics from those used in reference, 7 ranging widely in terms of construction and fiber type as shown in Table I. Their mechanical properties were already tested in that study following Kawabata's definitions and are provided in Table II.

We used the yarn pullout test (on warp yarns only) on these fabrics. Figure 5a is a typical pullout curve

TABLE I. Specifications of the fabrics.

No.	Fabric name	Fiber content	Weave	Fabric count, W × F (no./cm)	Fabric weight, g/m²
1	print	100% cotton	plain	28 × 28	106.24
2	print	100% cotton	twill	28 × 28	110.27
3	denim	100% cotton	twill	25 × 17	298.91
4	canvas	100% cotton	plain	28 × 17	307.88
5	flannel	100% cotton	plain	18 × 17	131.81
6	flannel	100% cotton	twill	18 × 12	289.17
7		100% wool	twill	12 × 12	256.69
9	gabardine	100% polyester	twill	26 × 18	221.17
10		35% wool 65% polyester	plain	17 × 15	195.55
11		50% polyester 50% rayon	twill	32 × 25	137.67
12		100% rayon	plain	42 × 31	115.72
13	taffeta (F*)[a]	100% silk	plain	48 × 40	49.94
14	taffeta (F*)	100% polyester	plain	38 × 37	81.44
15	taffeta (F*)	100% acetate	plain	36 × 20	122.21

[a] F* = filament yarns.

TABLE II. Test results for selected fabrics.

Fabric	P_{lm}, g	E_{lm}, g	2HB,[a] g/cm	MIU,[a] g	SMD,[a] g	LT[a]	WT,[a] g/cm^2	RT,[a] %	2HG,[a] g/cm	RC,[a] %	T,[a] mm
1	26.16	206.00	0.44	17.08	1.59	0.92	23.37	39.74	9.42	38.33	0.51
2	11.40	111.47	0.23	30.46	2.09	0.80	21.01	42.06	4.27	34.96	0.66
3	49.23	153.37	2.68	23.98	2.27	0.91	1.93	41.95	7.39	36.42	0.99
4	717.00	930.55	4.74	21.53	1.90	0.96	2.15	43.86	16.92	41.06	1.02
5	25.52	318.78	0.86	35.93	2.35	0.72	13.94	51.40	8.94	40.44	0.91
6	21.65	80.52	4.96	29.53	1.75	0.95	1.65	45.03	4.80	41.47	1.58
7	44.62	154.26	1.12	34.38	2.72	0.78	2.17	51.39	4.98	39.48	1.21
9	30.57	53.05	0.78	12.96	1.64	0.91	0.36	68.37	1.19	40.94	0.87
10	25.89	72.25	0.52	39.26	2.34	0.88	1.12	56.94	2.15	41.41	1.37
11	7.54	40.78	0.18	30.76	1.20	0.73	4.22	57.95	0.69	39.24	0.79
12	20.75	93.66	0.18	22.79	1.06	0.86	2.38	62.51	6.93	36.00	0.56
13	15.74	88.75	2.13	7.64	1.15	0.77	18.37	59.85	5.99	43.28	0.27
14	83.14	165.78	0.45	5.72	1.23	0.88	37.53	58.61	8.18	55.60	0.27
15	43.57	198.86	1.68	6.34	2.32	0.95	41.66	66.85	6.58	55.55	0.35

[a] Kawabata's parameter code [7].

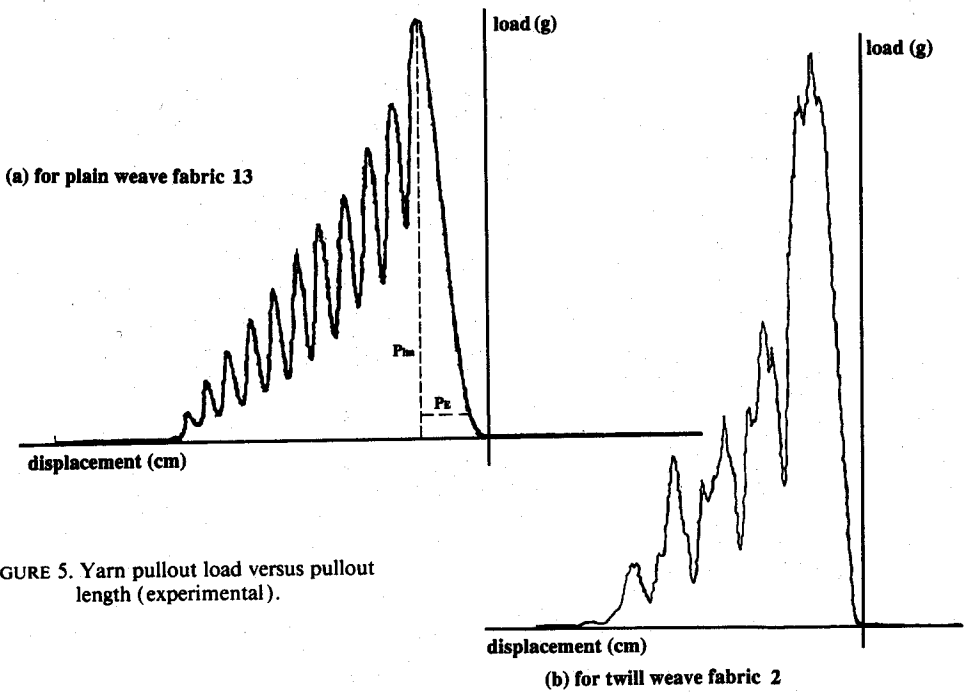

FIGURE 5. Yarn pullout load versus pullout length (experimental).

for a plain weave obtained experimentally using fabric 13, and Figure 5b is the result using twill fabric 2. We must stress here that what these curves show is pullout load versus pullout yarn length instead of embedded yarn length. This differentiates the nature of Figure 5 from Figures 3 or 4. Another difference between them is that in Figure 5, the stress level is not maintained. Consequently, there is a stress drop after the yarn is pulled out of each crossing point; the curves thus consist of peaks instead of steps as in Figures 3 and 4. Two parameters are obtained from each pullout curve, that is, the maximum pullout load P_{lm} and the nominal modulus of the curve $E_{lm} = \frac{P_{lm}}{P_E}$, with P_E being the nominal elongation as indicated in Figure 5a. The results for all fabrics are provided in Table II, and each of the data is the average of at least five test results.

Using the correlation analysis, possible connections between the two parameters from the curves and the corresponding fabric mechanical properties are then reflected through the values of the correlation coefficients in Table III. Noticing the difference in pullout behaviors between the twill structure and the plain weave, as illustrated in Figure 5, we have calculated the correlation coefficients separately for both fabric groups. Table III shows that the property most closely related to P_{lm} and E_{lm} for both twill and plain fabrics

TABLE III. Correlations between yarn pullout data and fabric properties.

	2HB	MIU	SMD	LT	WT	RT	2HG	RC	T
P_{lm}									
Plain	0.882	0.055	−0.075	0.333	−0.293	−0.483	0.837	−0.145	0.358
Twill	0.274	0.195	0.727	0.385	−0.524	−0.110	0.642	0.0	0.324
E_{lm}									
Plain	0.864	0.141	−0.084	0.190	−0.214	−0.593	0.916	−0.214	0.383
Twill	0.161	0.355	0.947	0.055	0.105	−0.653	0.886	0.499	0.176

is fabric shear hysteresis 2HG, as also depicted in Figures 6a and b of the relationship between 2HG and E_{lm} for both plain and twill fabric types, respectively. This is easy to explain, since yarn pullout behavior is mainly determined by yarn mobility within the fabric, which is just what 2HG represents. Also, there are high correlations between fabric bending hysteresis 2HB, tensile resilience RT, and the two yarn pullout parameters for plain and twill fabrics.

It is surprising that the fabric surface frictional coefficient MIU has barely any correlation with either P_{lm} or E_{lm}. But the other fabric surface property, surface roughness SMD, is highly correlated with E_{lm}, although for twill fabric only. This close relation between the two is illustrated in Figure 7. Further study is certainly desirable for more definite conclusions in terms of the connections between yarn pullout behavior and fabric properties.

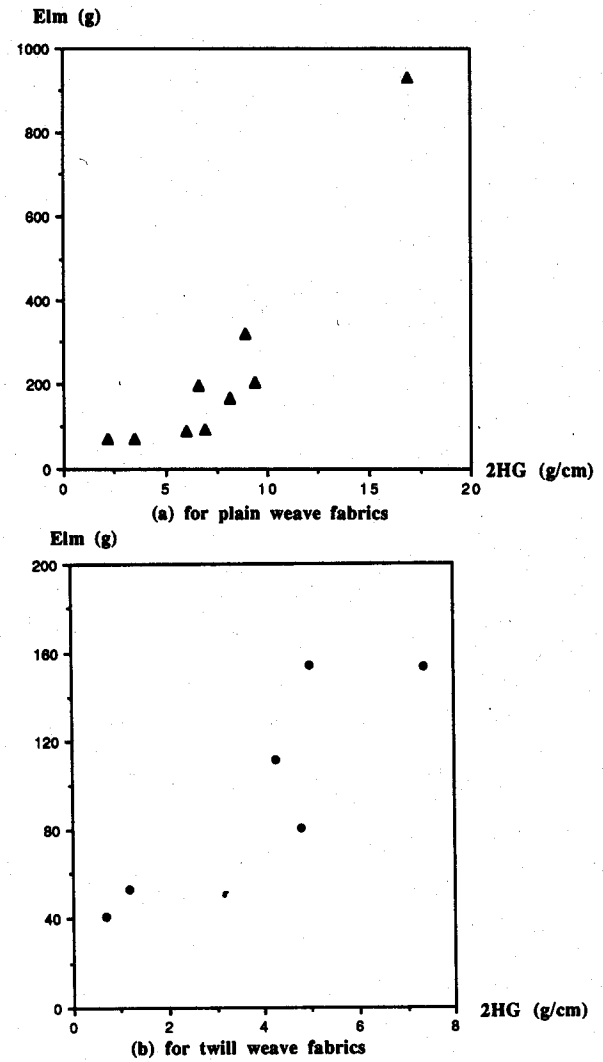

FIGURE 6. Relationship between 2HG and E_{lm}.

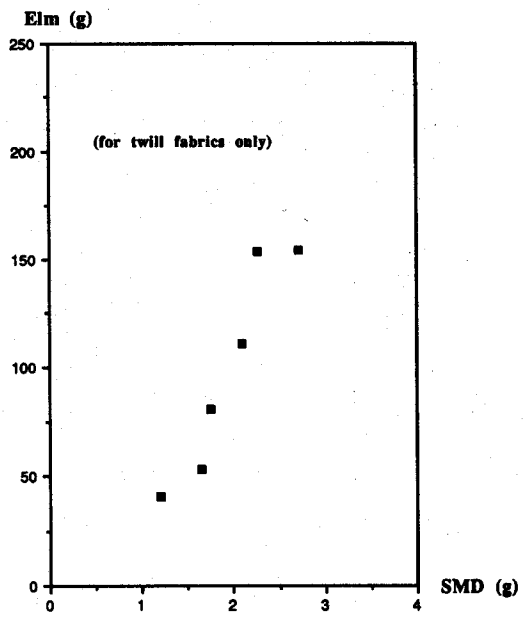

FIGURE 7. Relationship between SMD and E_{lm}.

COMPARISON OF PREDICTED AND MEASURED CRITICAL YARN LENGTHS

For practical applications, it is more convenient to use the nominal restraint force g_y as defined in Equation 7 than the equivalent shear strength τ_s of a crossing point. Also seen from its definition, this nominal restraint force g_y is a very critical system parameter, in-

cluding the geometric and mechanical properties of the yarns and representing the intensity of yarn interaction at a crossing point.

First of all, based on the experimentally determined pullout load P_{lm} and the fabric count in filling direction n_y, we can estimate for each fabric the restraint force g_y by rearranging Equation 4 into

$$g_y = \frac{P_{lm}}{Int(n_y L)\tanh \rho w_y} = \frac{P_{lm}}{Int(n_y L)\eta_y} \quad . \quad (12)$$

Just as an illustration, we use here only four of the fabrics listed in Table I. The calculated results of g_y for the four plain fabrics are shown in Table IV. In our calculation, we have chosen for all four fabrics $\frac{w_y}{t_y}$ = 2.0 by estimation and $\frac{G_y}{E_y}$ = 0.3 based on the result in reference 8, so we have η_y = 0.5498.

Once we have a g_y value, we can predict the slope of the yarn pullout curve using

$$\frac{dP_{lm}}{dL} = E_{lm} = Int(n_y) g_y \eta_y \quad . \quad (13)$$

Again the results are provided in Table IV. The trend of these predicted E_{lm} values is reasonably consistent with that of the experimentally determined results, given the fact that there is a slight difference between the two in definition: the theoretical value is the initial slope of the curve, and the experimental value is the average slope of the curve as shown in Figure 5a.

As indicated in Equation 11, there is a critical value L_c for a yarn length embedded in fabric beyond which the yarn will break within rather than be pulled out of the fabric. The value of L_c is determined by fabric and yarn properties. Equation 11 can in fact be simplified using Equations 5, 7, and 8 as

$$L_c = \frac{P_{lu}}{Int(n_y) g_y \eta_y} = \frac{P_{lu} L}{P_{lm}} \quad . \quad (14)$$

That is, the critical length L_c is proportional to the yarn breaking load P_{lu} and inversely proportional to the maximum pullout load P_{lm} at a given embedded yarn length L. The maximum pullout load P_{lm} when the embedded yarn length L = 0.6 cm and the yarn breaking load P_{lu} have been experimentally determined and are shown in Table IV. The results of critical yarn length L_c, both experimentally measured and theoretically predicted using Equation 14, for all four fabrics are also shown in Table IV. Given the complexity of yarn interactions during the pullout test and the factors we ignored in the assumptions in developing the theory, the predicted values are reasonably close to the experimental values, and the trend of both is consistent.

Conclusions

Since yarn interaction at crossing points is the only mechanism through which yarns in two orthogonal and otherwise isolated systems form an interlocked fabric system with fairly high strength, the yarn pullout test, by overcoming resistance at crossing points, is a very effective way to examine fabric properties both theoretically and experimentally. Besides yarn embedded length, the maximum pullout load is related to yarn geometric and mechanical properties and the corresponding fabric count. For different fabric weave structures and yarn types, yarn pullout behaviors are also different. The critical yarn embedded length is proportional to the yarn tensile breaking load and inversely proportional to the maximum yarn pullout force at a given embedded length.

Literature Cited

1. Bartos, P., Analysis of Pull-out Tests on Fibers Embedded in Brittle Matrices, *J. Mater. Sci.* **15,** 3122 (1980).
2. Cox, H. L., The Elasticity and Strength of Paper and Other Fibrous Materials, *Br. J. Appl. Phys.* **3,** 72 (1952).
3. Greszczuk, L. B., Theoretical Studies of the Mechanics of the Fiber-Matrix Interface in Composites, in "Interfaces in Composites," ASTM STP 452, 1969, p. 42.
4. Hsieh, C. H., Interfacial Debonding and Fiber Pullout Stresses of Fiber-reinforced Composites, *Mater. Sci. Eng.* **A123,** 1 (1990).
5. Kim, J. K., Baillie, C., and Mai, Y. W., Interfacial Debonding and Fiber Pull-out Stresses, Part I: Critical

TABLE IV. Experimental and predicted results for four fabrics.[a]

Fabric	n_y^e, no./cm	P_{lm}^e, g/6 mm	P_{lu}^e, g	g_y^p, g	E_{lm}^e, g/cm	E_{lm}^p, g/cm	L_c^e, mm	L_c^p, mm
1	28.0	26.16	304.77	2.84	206.00	43.62	125.00	65.99
4	16.9	717.00	799.05	128.38	930.55	1195.00	6.00	6.64
12	31.1	20.75	327.64	2.02	93.66	34.58	160.00	85.45
13	40.2	15.74	134.86	6.28	88.75	138.57	57.75	51.41

[a] Fabric specifications given in Table I, ^{e} = experimental results; ^{p} = predicted results.

Comparison of Existing Theories with Experiments, *J. Mater. Sci.* **27,** 3143 (1992).
6. Lawrence, P., Some Theoretical Considerations of Fiber Pull-out from an Elastic Matrix, *J. Mater. Sci.* **7,** 1 (1972).
7. Pan, N., Zeronian, H., and Ryu, H., An Alternative Approach to the Objective Measurement of Fabrics, *Textile Res. J.* **63,** 33 (1993).
8. Pan, N., Development of a Constitutive Theory for Short Fiber Yarns: Mechanics of Staple Yarn Without Slippage Effect, *Textile Res. J.* **62,** 749 (1992).
9. Pan, N., Theoretical Modeling and Analysis of Fiber Pull-Out Behavior from a Bonded Fibrous Matrix: Elastic Bond Case, *J. Textile Inst.* (in press).
10. Realff, M. L., Seo, M., Boyce, M. C., Schwarz, P., and Backer, S., Mechanical Properties of Fabrics Woven from Yarns Produced by Different Spinning Technologies: Yarn Failure as a Function of Gauge Length, *Textile Res. J.* **61,** 517 (1991).
11. Sebastian, S. A. R. D., Bailey, A. I., Briscoe, B. J., and Tabor, D., Effect of a Softening Agent on Yarn Pull-out Force of a Plain Weave Fabric, *Textile Res. J.* **56,** 604 (1986).
12. Sebastian, S. A. R. D., Bailey, A. I., Briscoe, B. J., and Tabor, D., Extensions, Displacements and Forces Associated with Pulling a Single Yarn from a Fabric, *J. Phys. D. Appl. Phys.* **10,** 130 (1987).
13. Taylor, H. M., Tensile and Tearing Strength of Cotton Cloths, *J. Textile Inst.* **50,** T161 (1959).

Manuscript received January 15, 1993, accepted March 5, 1993.